

Small-x QCD and forward physics results from CMS

Gábor I. Veres*

CERN

E-mail: gabor.veres@cern.ch

The CMS Collaboration has a comprehensive program of small-x QCD and forward physics measurements, which is supported by an excellent experimental coverage into the very forward phase space. Some of the highlights in terms of testing QCD at low transverse momenta (p_T) and at high pseudorapidities (η) with jets and charged particles are summarized. Also extremely rare processes, as the measurement of exclusive W-pair production in photon-photon collisions in proton-proton (pp) data are discussed. The range of physics results is complemented by studies of diffractive collisions, as well as of multi-parton interactions and soft-QCD phenomena. The measurement of the underlying event at different center-of-mass energies is another fundamental result presented. First results based on the data collected at 13 TeV are also discussed.

*The European Physical Society Conference on High Energy Physics
22-29 July 2015
Vienna, Austria*

*Speaker.

The Standard Model of particle physics is a remarkably successful theory to describe and predict the properties of interactions at small length scales. The large coupling and self-interacting nature of Quantum Chromodynamics (QCD), representing the theory of the strong interaction, encompasses various areas and phenomena, where first-principles calculations are exceedingly difficult or not even possible. A large variety of phenomenological models and a number of experimental measurements are aiming at a better understanding of these non-perturbative processes. These are not only profoundly important because they are responsible for a very large fraction of the total cross section of hadron-hadron collisions at high energies, but they are also indispensable ingredients of improving background estimates in case of precise searches for new phenomena beyond the Standard Model. Examples of such measurements to be presented here are single- and double-diffraction phenomena and cross sections, searches for signs of double parton scattering (in four-jet events with two b-jets), features of the underlying event and its dependence on the hard scale present in the collision and on the center-of-mass energy, and particle production at low p_T . The emission source size of the latter is studied in terms of Bose-Einstein correlations. In addition, a search for signs of anomalous quartic gauge couplings are presented using exclusive WW events.

The CMS experiment is ideally suited to carry out the above mentioned studies. The central feature of the CMS apparatus is a superconducting solenoid of 6 m internal diameter. Within the magnet volume are the silicon pixel and strip tracker, the crystal electromagnetic calorimeter, and the brass and scintillator hadron calorimeter. Muons are measured in gas-ionization detectors embedded in the steel flux-return yoke of the magnet. The tracker measures charged particles within $|\eta| < 2.4$. It has 1440 silicon pixel and 15 148 silicon strip detector modules, arranged in 14 tracking layers. The barrel region of the CMS pixel detector consists of three layers very close to the beamline. In addition to the barrel and endcap detectors, CMS has extensive forward calorimetry. The forward component of the hadron calorimeter, HF ($2.9 < |\eta| < 5.2$), consists of

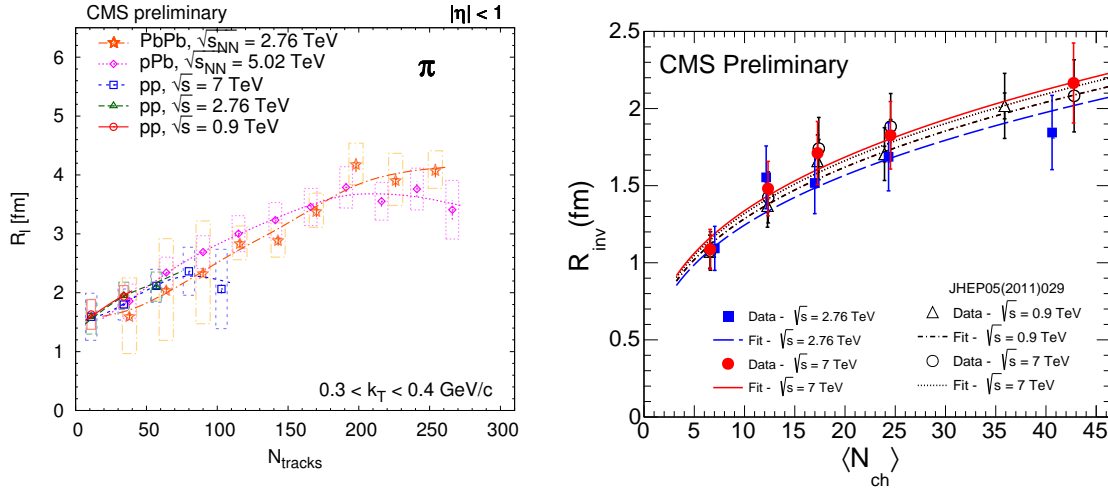


Figure 1: Left: N_{tracks} -dependence of the three-dimensional pion radii (the R_l component), shown here for $0.3 < k_T < 0.4$ GeV/c, for all studied reactions. Lines are drawn to guide the eye. Right: R_{inv} is shown as a function of the charged particle multiplicity, N_{ch} , for pp collisions at 2.76 TeV and 7 TeV. Outer error bars the statistical and systematic uncertainties added in quadrature.

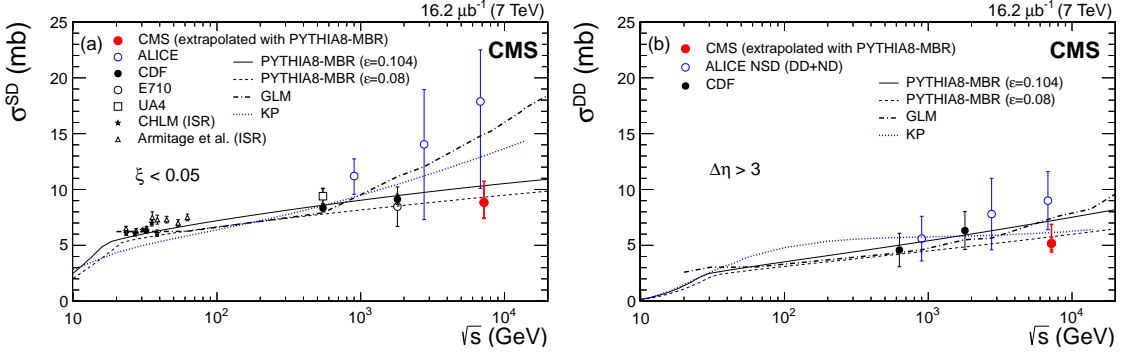


Figure 2: Diffractive cross sections as a function of collision energy measured in pp and $p\bar{p}$ collisions compared to model predictions. Left: total single diffractive (SD) cross section for $\xi < 0.05$. Right: total double diffractive (DD) cross section for $\Delta\eta > 3$. The inner (outer) error bars of the CMS data points correspond to the statistical and systematic (and the additional extrapolation) uncertainties added in quadrature.

steel absorbers with embedded radiation-hard quartz fibers, providing fast collection of Cherenkov light. The very forward angles are covered at one end of CMS ($-6.6 < \eta < -5.2$) by the CASTOR calorimeter, made of quartz plates embedded in tungsten absorbers, segmented in 16 ϕ -sectors and 14 z -modules. A detailed description of the CMS detector can be found in [1].

Low momentum particles detected after each pp collision appear to be emitted from a source with a finite size. Correlations between identical bosons with a small relative momentum can be used to investigate the dependence of the emission source size on various quantities, e.g. the charged particle multiplicity in the collision. These studies were carried out both with identified [2] and non-identified particles [3], with slightly different, complementary methods. As an example, in case of identified particles, the following function was fit to the three-dimensional two-particle correlation, where $q_{l,o,s}$ are relative momentum components in the longitudinally co-moving system of the particle pair: $1 + \lambda \exp[-\sqrt{q_l^2 R_l^2 + q_o^2 R_o^2 + q_s^2 R_s^2}]$. The left panel of Fig. 1 shows R_l as a function of multiplicity measured in pp , pPb and $PbPb$ collisions at various \sqrt{s} values. In case of the non-identified particles, the fit function to the one-dimensional correlation, where Q_{inv} is the invariant relative momentum of the particle pair, was: $C[1 + \lambda \exp^{-(Q_{inv} R_{inv})^a}](1 + \delta Q_{inv})$. The behavior R_{inv} in pp collisions at 2.76 TeV and 7 TeV is investigated as a function of multiplicity as shown on the right panel of Fig. 1. The increase of R_{inv} with N_{ch} shows a scaling property of the lengths of homogeneity with increasing collision center-of-mass energy.

Diffractive dissociation processes in pp collisions at 7 TeV were studied in events with a large rapidity gap in the detector. The single- (SD) and double- (DD) diffractive processes have been separated utilizing the CASTOR calorimeter. The cross sections were measured as a function of the masses M_X and M_Y of the hadronic systems on the two sides of the rapidity gap. The differential cross sections are integrated over the measurable M_X and M_Y regions, and extrapolated to the full phase space to obtain the total SD and DD cross sections. This extrapolation, which amounts to approximately a factor of 2, was carried out using the PHYTIA 8 MBR event generator tune, after an extensive set of comparisons between this model and the experimental data. The extrapolated SD and DD cross sections thus obtained are $\sigma^{SD} = 8.84 \pm 0.08(\text{stat})_{-1.38}^{+1.49}(\text{syst})_{-0.37}^{+1.17}(\text{extrap})$ mb and $\sigma^{DD} = 5.17 \pm 0.08(\text{stat})_{-0.57}^{+0.55}(\text{syst})_{-0.51}^{+1.62}(\text{extrap})$ mb, respectively [4], and shown on Fig. 2

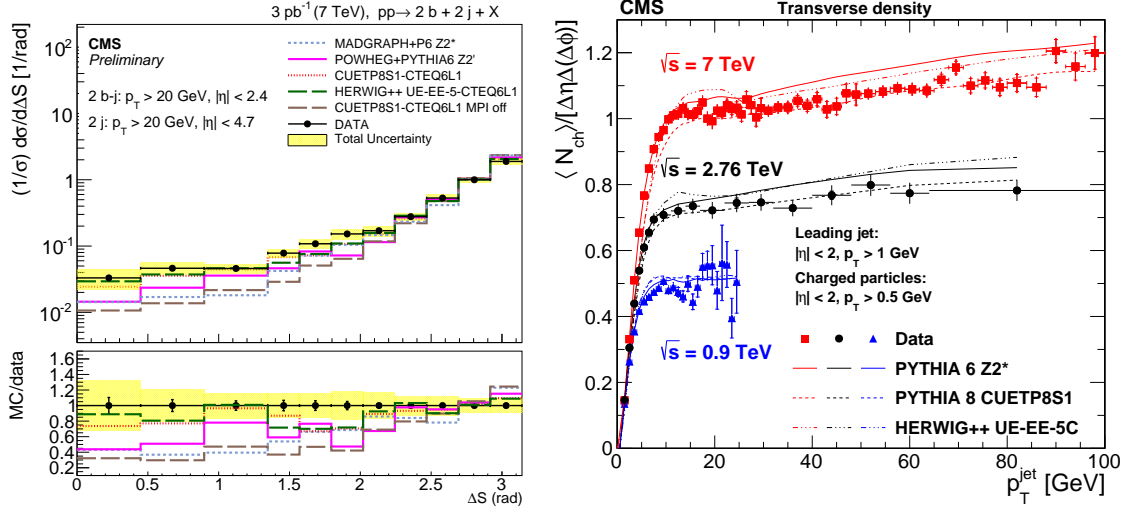


Figure 3: Left: Normalized cross sections unfolded to the stable particle level as a function of ΔS , compared to predictions of the POWHEG, MADGRAPH, PYTHIA 6, PYTHIA 8 and HERWIG++ models. A comparison with the PYTHIA 8 CUETP8S1-CTEQ6L1 predictions without the simulation of multi-parton interactions is also shown. The lower panel shows the ratios of the predictions to the data. The yellow band represents the total uncertainty. Right: Comparison of the particle density in the underlying event in the transverse region at $\sqrt{s} = 0.9, 2.76,$ and 7 TeV, as a function of p_T^{jet} . The data (symbols) are compared to various MC simulations (curves).

compared to other measurements and models as a function of \sqrt{s} . These results are consistent with a weakly rising trend as a function of center-of-mass energy, as also predicted by the models.

At high center-of-mass energies the gluon densities become large at low x values. Hence, the probability to have more than one partonic interaction becomes non-negligible, leading to the production of pairs of different flavored jets via double parton scattering (DPS). The cross section of the production of two jets and two b-jets, as well as a production of three jets in addition to an energetic photon in pp collisions at 7 TeV has been measured to gain experimental access to this phenomena. In case of the study of four jet events, a variable ΔS was defined as the azimuthal angle between the light jet pair and the b-jet pair, where the direction of a jet pair is defined by the vector sum of their transverse momenta. The measured cross section as a function of ΔS is shown on the left panel of Fig. 3. The data are not well described by the models, underestimate the region at values of $\Delta S < 2$, and do not follow well the decreasing shape towards lower values, showing the need for MPI contributions in the simulation [5].

A measurement of the underlying event (UE) activity in proton-proton collisions at 2.76 TeV center-of-mass energy was also performed recently using events with charged-particle jets produced in the central pseudorapidity region ($|\eta^{\text{jet}}| < 2$). The UE activity is measured in the azimuthal region transverse to the direction of the highest p_T jet. The center-of-mass energy dependence of the UE activity in the transverse region is presented on the right panel of Fig. 3 as a function of p_T^{jet} for $\sqrt{s} = 0.9, 2.76,$ and 7 TeV. A fast rise with increasing center-of-mass energy of the activity in the transverse region is observed for the same value of the leading charged-particle p_T^{jet} . All presented model tunes predict a center-of-mass energy dependence consistent with that of

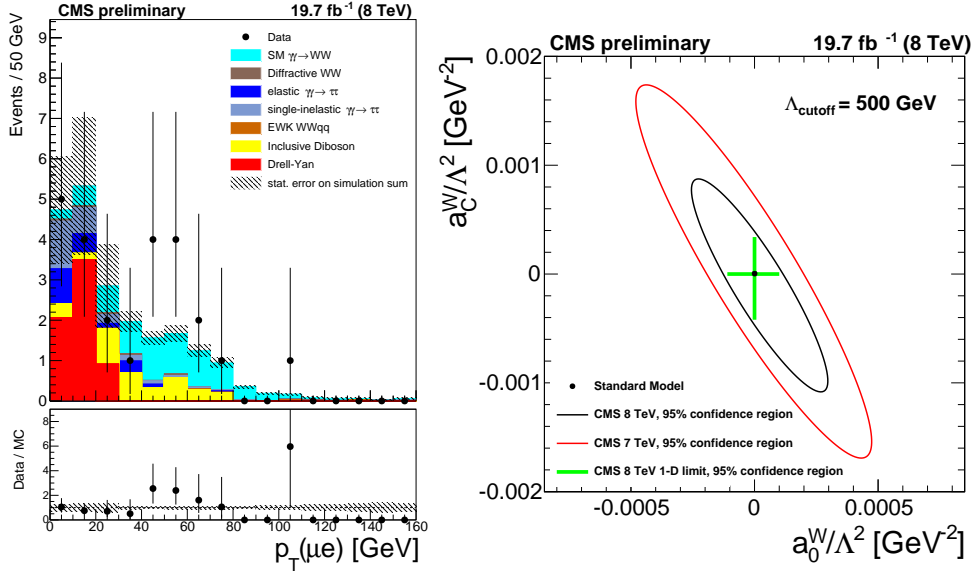


Figure 4: Left: muon-electron transverse momentum distribution for events with zero associated tracks. Right: excluded values of the anomalous coupling parameters a_0^W/Λ^2 and a_C^W/Λ^2 with $\Lambda_{\text{cutoff}} = 500$ GeV. The area outside the solid contour is excluded by this measurement at 95% CL. The predicted cross sections are rescaled to include the contribution from proton dissociation.

the data [6].

A search for (quasi)exclusive $\gamma\gamma \rightarrow W^+W^-$ processes in pp collisions at 8 TeV was carried out using data corresponding to 19.7 fb^{-1} integrated luminosity. Events were selected by requiring an electron-muon pair with large transverse momentum $p_T(\mu^\pm e^\mp) > 30 \text{ GeV}/c$ and no other charged particles detected from the same collision point. After all event selection cuts, 13 events are observed over an expected background of 3.5 ± 0.5 events, corresponding to an excess of 3.6σ over the background-only hypothesis. This event yield is compatible with the Standard Model prediction. The dilepton transverse momentum spectrum, shown on the left panel of Fig. 4, is studied for deviations from the Standard Model, and the resulting upper limits are compared to predictions assuming genuine anomalous quartic gauge couplings of dimension-6 with two parameters, a_0^W/Λ^2 and a_C^W/Λ^2 , where Λ is the scale of new physics. Two-dimensional limits were obtained in the $a_0^W/\Lambda^2, a_C^W/\Lambda^2$ parameter space using a dipole form factor with a cutoff scale $\Lambda_{\text{cutoff}} = 500$ GeV to avoid unitarity violation. The resulting two dimensional 95% confidence region is shown on the right panel of Fig. 4 and compared to the earlier 7 TeV result from CMS [7].

Finally, the first physics results obtained at the LHC at 13 TeV are presented, namely the pseudorapidity distribution of charged hadrons in pp collisions. The CMS detector operated at zero magnetic field. The yield of charged hadrons produced in inelastic pp collisions was determined in the central region of the CMS pixel detector ($|\eta| < 2$) using both hit pairs and reconstructed tracks. The η distribution of charged hadrons can be seen on the left panel of Fig. 5 [8]. For central pseudorapidities ($|\eta| < 0.5$), the charged-hadron multiplicity density is $5.49 \pm 0.01(\text{stat}) \pm 0.17(\text{syst})$. The result is compared to predictions from Monte Carlo event generators and to similar measurements made at lower collision energies on the right panel of Fig. 5. In the central region, the measured $dN_{ch}/d\eta$ distribution is consistent with predictions of the PYTHIA8 (tunes CUETP8S1 and

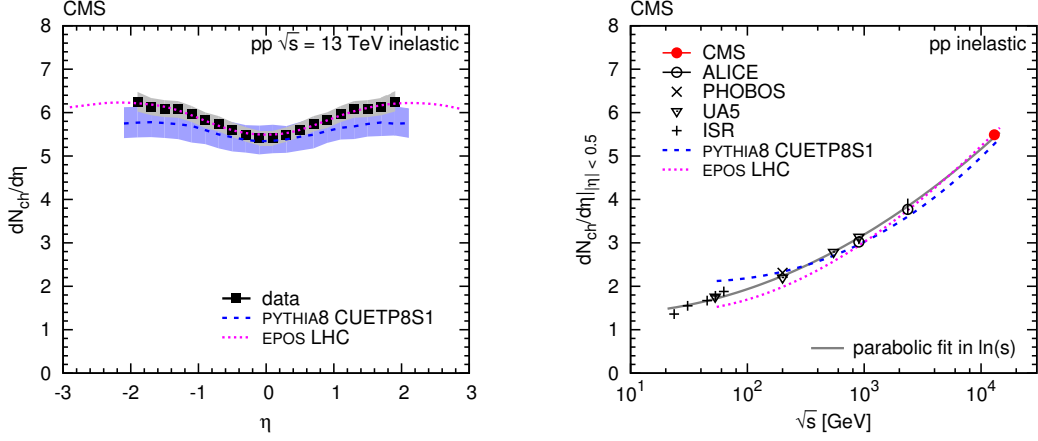


Figure 5: Left: Distributions of the pseudorapidity density of charged hadrons in the region $|\eta| < 2$ in inelastic pp collisions at 13 TeV compared to the PYTHIA8 CUETP8S1 and the EPOS LHC models. Right: Center-of-mass energy dependence of $dN_{ch}/d\eta$ including measurements at lower center-of-mass energy. The solid curve is a second-order polynomial fit in $\ln(s)$.

CUETP8M1) and EPOS LHC event generators, while those in a wider η range are better described by the latter model. These results provide new constraints for the improvement of perturbative and nonperturbative QCD aspects implemented in hadronic event generators.

In summary and outlook, the CMS Collaboration has a versatile and active forward, diffractive, exclusive, soft QCD, MPI and low- x physics program, which is facilitated by the unique forward instrumentation. In addition, a joint physics program and data collection is underway with the TOTEM experiment, with an outlook to tagging diffractive and central-exclusive processes at high luminosity with a new Precision Proton Spectrometer. In the present talk, various recent results concerning Bose-Einstein correlations, diffractive cross sections, four-jet cross sections, underlying event properties, new limits on anomalous quartic gauge couplings have been reviewed, together with the first physics results at the highest-ever LHC energy on charge particle pseudorapidity distributions.

References

- [1] S. Chatrchyan *et al.* [CMS Collaboration], JINST **3** (2008) S08004.
- [2] CMS Collaboration, CMS-PAS-HIN-14-013 (2014).
- [3] CMS Collaboration, CMS-PAS-FSQ-13-002 (2014)
- [4] V. Khachatryan *et al.* [CMS Collaboration], Phys. Rev. D **92**, no. 1, 012003 (2015)
- [5] CMS Collaboration, CMS-PAS-FSQ-13-010 (2015)
- [6] V. Khachatryan *et al.* [CMS Collaboration], JHEP **1509**, 137 (2015)
- [7] S. Chatrchyan *et al.* [CMS Collaboration], JHEP **1307**, 116 (2013)
- [8] V. Khachatryan *et al.* [CMS Collaboration], arXiv:1507.05915 [hep-ex].